Ritonavir Form III: A New Polymorph After 24 Years

Xin Yao[1,3], Rodger F. Henry[2], Geoff G. Z. Zhang[3,*]

[1] School of Pharmacy, University of Wisconsin-Madison, Madison, WI, 53705, USA

[2] Structural Chemistry, Research and Development, AbbVie Inc., North Chicago, IL, 60064, USA

[3] Development Sciences, Research and Development, AbbVie Inc., North Chicago, IL, 60064, USA

ABSTRACT:

Polymorphism occurs widely in pharmaceutical solids, and must be thoroughly studied during product development. Twenty-four years after ritonavir (RTV) Form II materialized, we report a new polymorph, Form III, discovered via melt crystallization. Form III has a unique PXRD pattern, Raman spectrum, lower melting point and heat of fusion, compared to the known polymorphs, Form I and Form II. It is the least stable form, monotropically, among the three polymorphs. Form III differs from Form I and Form II in conformation and hydrogen bonding motifs. Nucleation from RTV supercooled liquid is slow, and selected Form III exclusively. The discovery of RTV Form III demonstrates the importance of crystal nucleation studies. Crystallization from supercooled liquids should be incorporated as part of polymorph screening workflow.

Keywords:

Ritonavir; Polymorphism; Melt crystallization; Crystal nucleation; Crystal Structure; Polymorph selection

INTRODUCTION

The same compound can exist in different crystal structures possessing different physicochemical properties. This phenomenon is known as polymorphism and widely occurs for pharmaceuticals.[1-4] Due to their different molecular conformation or crystal packing, different polymorphs can exhibit very different pharmaceutically relevant properties, such as solubility, dissolution rate, and stability.[4] Thus, polymorphism of a pharmaceutical agent needs to be well understood and carefully controlled during product development.

Ritonavir (RTV), a protease inhibitor marketed as Norvir®, is an antiviral drug active against human immunodeficiency virus (HIV).[5] Its molecular structure is shown in Scheme 1. Being a strong cytochrome P450 3A (CYP3A) inhibitor, ritonavir interacts with many other drugs that are primarily metabolized by CYP3A leading to mutually increased exposures.[5] This pharmacokinetic boosting property was utilized in many other antiretroviral (e.g. Kaletra®,[6] Aptivus®,[7] Reyataz®.[8]) and Hepatitis C treatment therapies (e.g. Viekira PAK®.[9]). Most recently it was included in Paxlovid™,[10] a COVID-19 treatment that is active against viral protease M^{PRO}, as a pharmacokinetic boosting agent.

Ritonavir was discovered at Abbott Laboratories and introduced to the market in 1996. It is well known in the pharmaceutical industry, particularly among the solid-state community, for its unexpected development of a more stable polymorph Form II, in mid-1998, leading to the discontinuity of the marketed formulation.[11, 12] Although finding the most stable polymorph is important in drug product development as demonstrated by the RTV case, discovering/characterizing all crystal forms and understanding the solid-state landscape are also important, especially for subjects like structure-property relationship and polymorph prediction. In the decades since, polymorph screening has become an essential activity for drug product development of new chemical entities. Considerable investments have gone into research on new experimental approaches and computational prediction. In solution, polymorph screening is performed by varying solvent selection, pH, concentration gradients, temperature, agitation, etc., either manually or in a high-throughput fashion.[13] Additionally, crystallization from the melt for discovering new polymorphs, especially metastable polymorphs, is getting more attention.[14-16] Other screening methods can be performed by introducing crystalline substrates,[17] polymers,[18] high pressures or vacuum,[19] space confinement,[20] and liquid/vapor interface.[21] Besides the

experimental methods, many successful examples of computational crystal structure prediction (CSP) demonstrate its ability to predict unknown crystal forms.[14, 22, 23]

Twenty-four years after RTV Form II materialized, we herein report a new polymorph, Form III, discovered via melt crystallization. We, serendipitously, discovered Form III in an effort to study crystal nucleation of amorphous RTV. This new polymorph was then characterized by powder X-ray diffractometry (PXRD), Raman spectroscopy, and differential scanning calorimetry (DSC). Single crystals were grown using a unique method, and the crystal structure was solved. Form III is the least stable, monotropically, and the least dense among the three polymorphs. It differs from Form I and Form II in conformation and hydrogen bonding motifs. The discovery of Form III emphasizes the importance of melt crystallization and crystal nucleation in polymorph discovery.

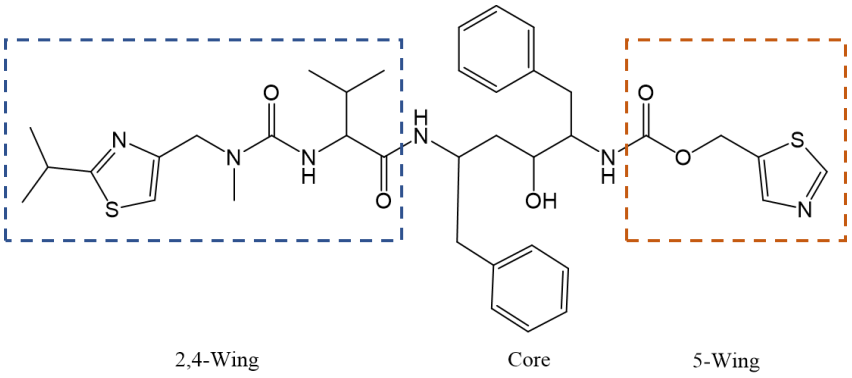

Scheme 1. Molecular structure of ritonavir (RTV).

EXPERIMENTAL SECTION

Ritonavir (RTV) Form II was used as received from AbbVie. Form I was prepared by adding RTV ethanol solution (100 – 200 mg/ml) into water. The ethanol solution was prepared by dissolving Form II RTV in ethanol at 50 °C with stirring. The solution was then filtered while hot and reheated to 50 °C to avoid any undissolved Form II. The hot solution was added into water quickly with stirring at 37 °C. After 2 days, the precipitated solid, Form I, was collected and dried under vacuum. Form III was prepared from the melt of RTV. Form II solids were melted on a glass coverslip (d = 22 mm) at 130 °C and covered with another coverslip to seal the melt. The "sandwich sample" was nucleated at 60 °C for 2 days, and then fully crystallized into Form III at 90 °C for 2 days.

Differiancial Scanning Calorimetry (DSC) was performed with a TA DSC2500 under 50 mL/min N_2 purge. Each sample was 1 – 3 mg, placed in an aluminum pan, heated to 90 °C at

10 °C/min, and then to 130 °C at 1 °C/min. PXRD data were collected using an ARL EQUINOX 3500 (Thermo Fisher Scientific Inc., Waltham, MA, USA) equipped with a CPS 590 detector and a Cu microfocus source. The diffractometer was operated at 40 kV and 40 mA. PXRD data were collected from 0 – 90° 2θ with an integration time of 1800 s. Raman microscopy was performed using an inVia Basis Raman Microscope (Renishaw, UK), coupled with a Leica DM 2500 confocal microscope and a 514 nm excitation Argon ion laser. Spectra were acquired in the range 1900 – 300 cm^{-1}. The spectra were collected using the static mode with 1 – 2 s exposure time, 10 – 100% light power, and 2 – 15 times scan based on the signal/noise ratio.

Single Crystal X-Ray Diffraction was used to solve the structure of RTV Form III. A single crystal of Form III was grown using the ”small droplet method”[24] as follows: RTV containing 10% Span 80 was prepared by milling first. Span 80 was added to enhance mobility and thus crystal growth rate of RTV in the molten state.[25] A small amount of RTV/Span was placed on a glass coverslip and melted at 403 K. The melt droplet was then cooled to 373 K and seeded with Form III crystal. Afterwards, the droplet was heated to ~ 388 K until one crystal piece was left as the perfect seed. Then, the seed was grown in the range of 363-373 K until the shortest dimension of the crystal was greater than 20 μm. All processes were performed on a hot stage with N_2 purge to prevent decomposition. The Form III single crystal is needle-like and can be separated from the melt with a tip at 373 K. A fragment of single crystal was harvested from the coverslip it was grown on. The crystal was mounted on polymer loop for data collection. The loop containing the crystal was mounted on a Bruker diffractometer equipped with a PHOTON II detector. Data were collected using Cukα radiation produced by a sealed tube. The structure was solved using intrinsic phasing and refined with shelxtl. All non-hydrogen atoms were refined anisotropically. Hydrogen atoms were included in calculated riding positions. Significant disorder was present in both wings of the structure, requiring the extensive use of constraints in the refinement.

RESULTS AND DISCUSSION

RTV Form III was crystallized from the melt. It was designated Form III following the two polymorphs (Form I and Form II) with known crystal structures. PXRD patterns of Form III show characteristic peaks at multiple 2θ angles (e.g., 7.8°, 13.0°, and 14.9°), see Figure 1, conforming a new polymorph of RTV. Form I and II powder patterns were collected as well for comparison.

They match the predicted patterns of solved structures in CSD data base, verifying the solid forms used in this study.

Three polymorphs of RTV can also be distinguished by their Raman spectra. Raman spectra of three polymorphs and amorphous RTV (glass) were collected and shows significant difference in the shaded area (1700–1650 and 1000–800 cm^{-1}) in Figure 2.

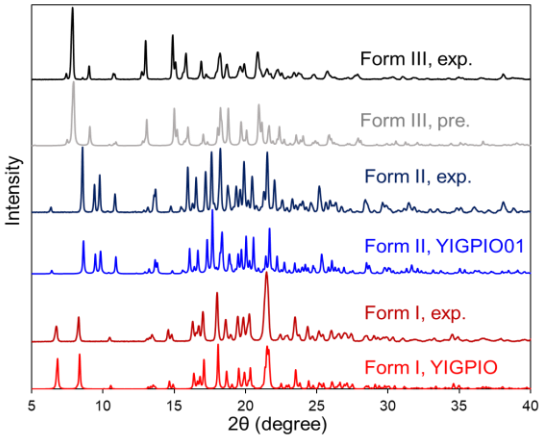

Figure 1. PXRD patterns of RTV polymorphs compared with the predicted patterns using crystal structures.

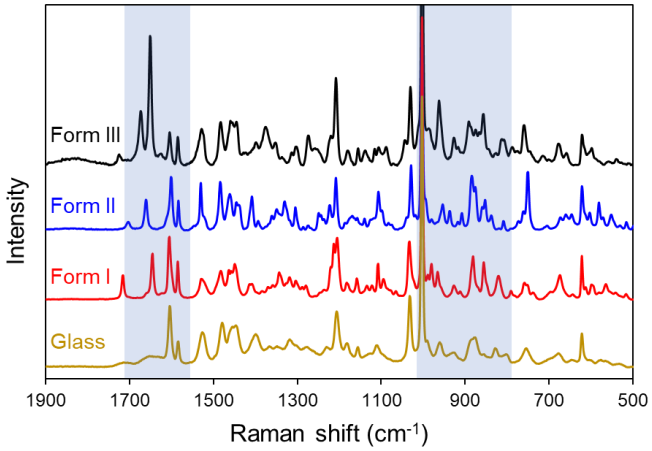

Figure 2. Raman spectra of RTV polymorphs and amorphous RTV.

To understand the thermodynamic stability relationship among the three polymorphs, the melting points (T_ms) and heats of fusion (ΔH_ms) were determined using DSC. The DSC thermograms of the three polymorphs are shown in Figure 3. Melting points and heats of fusion were tabulated in Table 1. Form III has the lowest T_m and ΔH_m, indicating it is the least stable polymorph among the three, monotropically, according to Burger and Ramberger's Heat of Fusion Rule.[26] Quantitatively, the free energy differences were calculated using the thermal fusion data and the equation $\Delta G_{liquid\text{-}crystal} = \Delta H_m (T_m – T) / T$. The free energy phase diagram was

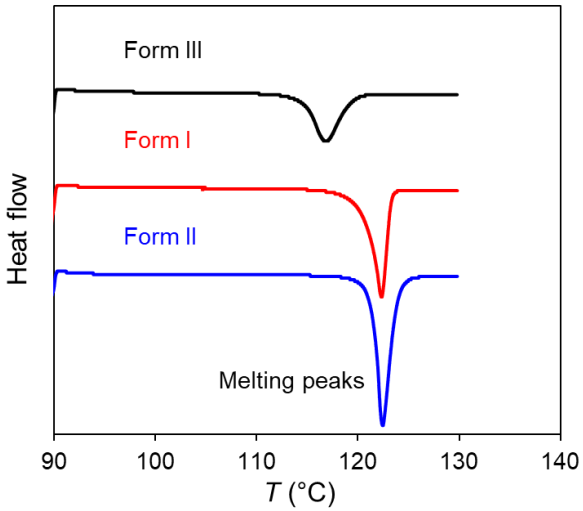

Figure 3. DSC thermograms of RTV polymorphs.

plotted in Figure 4a. Based on the free energy phase diagram, three polymorphs are, indeed, monotropically related; Form III being the least stable, and Form II being the most stable, across at all temperatures.

Knowing the free energy differences among the polymorphs allows the calculation of relative solubility among the polymorphs using the equation, $S_1 = S_2 \exp(\Delta G_{2\rightarrow1} / RT)$; where S_1 and S_2 are solubilities of the two phases, ΔG is the difference of the Gibbs free energy between the two phases, R is the gas constant, and T is temperature (K). The solubility ratios relative to Form II are calculated at 5, 25, and 37 °C, and plotted in Figure 4b. The horizontal dotted line in Figure 4b is the solubility ratio derived from experimental measurements in ethanol:water (99:1) solution, at 5 °C,[12] indicating consistency between experimental data and thermodynamic calculations.

In ethanol:water 99:1 solution, at 5 °C, solubility of Form III is calculated to be 695 – 744 mg/ml (based on solubility values of Form I and II, Table 1).[12] Such high solubility implies that Form III is unlikely to crystallize from solution, because it is extremely challenging to generate supersaturation for Form III. On the contrary, driving forces for nucleation and crystallization always exist for all polymorphs in the amorphous phases.

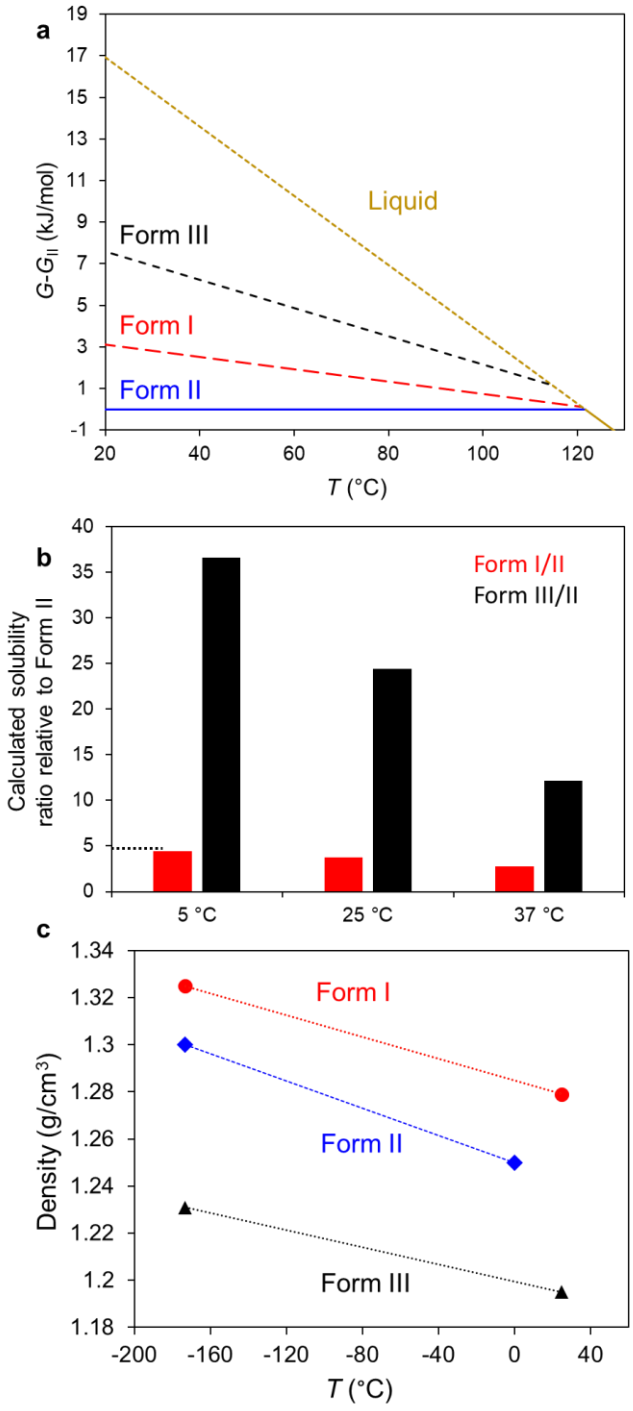

Figure 4. The Gibbs free energy, calculated solubility ratio relative to Form II, and density of RTV polymorphs.

Table 1. Relevant physical properties of RTV polymorphs.

	T_m (°C)[a]	ΔH_m (J/g)[a]	Solubility in ethanol/water (99/1) at 5 °C (mg/ml)	Thermal expansion coefficient (TEC) (ppm/K)
Form I	120.8 ± 0.0	74.8± 1.2	90[b]	178
Form II	121.5 ± 0.0	91.2 ± 1.4	19[b]	226
Form III	114.6 ± 0.2	53.1 ± 1.0	695[c] – 744[d]	150

[a] Analyses were performed using sigmoidal baseline.

[b] From Ref. 12.

[c] and [d] Calculated from the Form II and I solubility respectively.

Form III crystal structure was determined using single X-ray diffraction. The crystallographic data of Form III are shown in Table 2; molecular conformation is shown in Figure 5; hydrogen bonding motifs are shown in Figure 6; and hydrogen bond parameters in Table 3, together with those of Form I and Form II.

The three polymorphs have different conformations, as shown in Figure 5. By overlaying the core of RTV molecule in three polymorphs, the orientations of the wings are drastically different. Form III adopt the trans conformation in the N-methyl urea group of the 2,4-wing, as in Form II; and the trans conformation in carbamate group of the 5-wing, as in From I. The two groups can be both H-bonds donor and acceptor. These differences in conformation may impact hydrogen bonding motifs. Besides these major differences, Form III has the same phenyl position (in the middle of the core) as in Form II, and different rotation from Form II in the 2,4-wing. These conformational differences highlight the flexibility of RTV molecule.

Hydrogen bonding in RTV Form III consists of two modes as shown in Figure 6. The amide, carbamate, and urea groups all form N-H···O=C hydrogen bonds along the b-axis through translation. In the second mode the alcohol acts as a donor to the nitrogen of the thiazole ring in the 5-wing. This second mode extends parallel to the a-axis. The two modes combine to form a 2-dimensional hydrogen bonding network. Form III's hydrogen bonding is very similar to that seen in Form I. All of the hydrogen bonding pairs in both structures are identical. In Form I, however, all the hydrogen bonds propagate parallel to the b-axis, forming a 1-dimentional hydrogen bonding ribbon. RTV Form II also forms a 1-dimentional hydrogen bonding motif. But it forms a chain rather than a ribbon. The 2-dimentional hydrogen bonding motif is unique to Form III, with the other two known forms exhibiting one dimensional hydrogen bonding motifs.

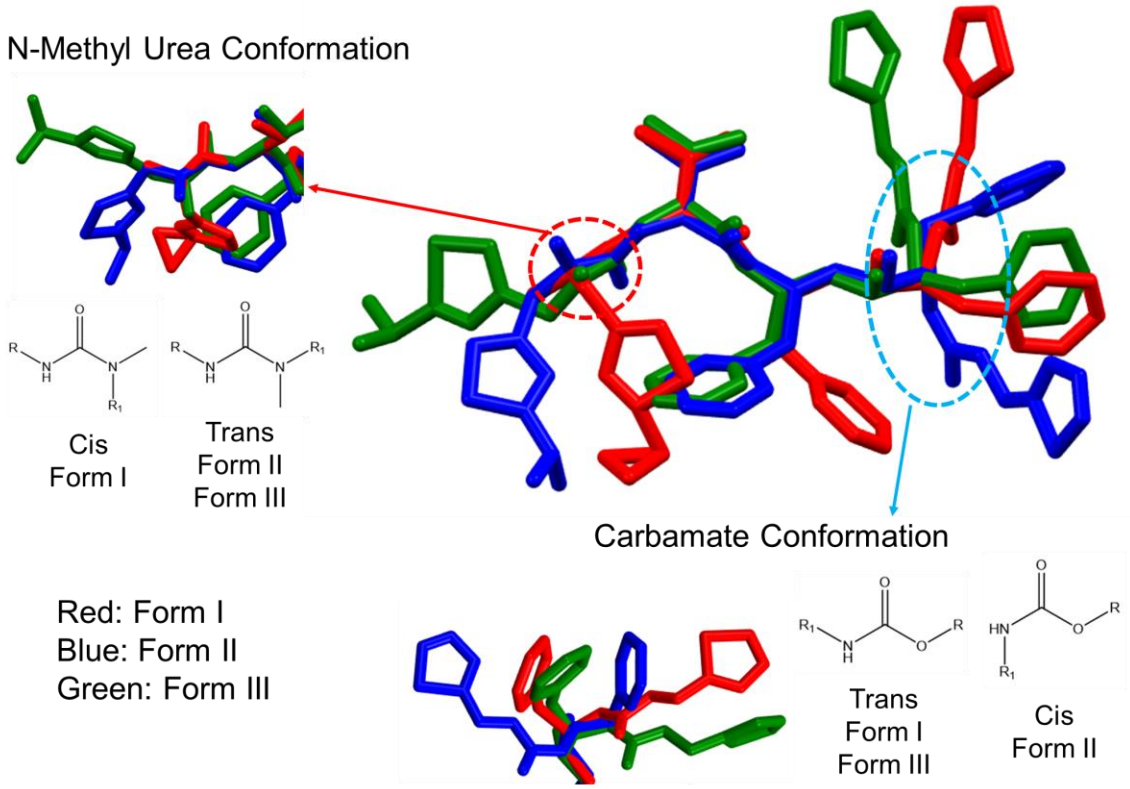

Figure 5. Molecular conformations in RTV polymorphs.

Table 2. Crystallographic information of RTV polymorphs at 100 K.

	Form III	Form I (YIGPIO02)	Form II (YIGPIO03)
a	23.3307(19)	13.344(2)	9.831(6)
b	4.9511(5)	5.215(<1)	18.485(11)
c	33.638(3)	26.693(4)	20.261(12)
alpha	90	90	90
beta	91.274(6)	103.46(<1)	90
gamma	90	90	90
volume	3884.6(6)	1806.5(6)	3682(4)
Z	4	2	4
Z’	1	1	1
Space group	C2	P21	P212121

Figure 6. Hydrogen bonding motifs in RTV polymorphs.

Form III

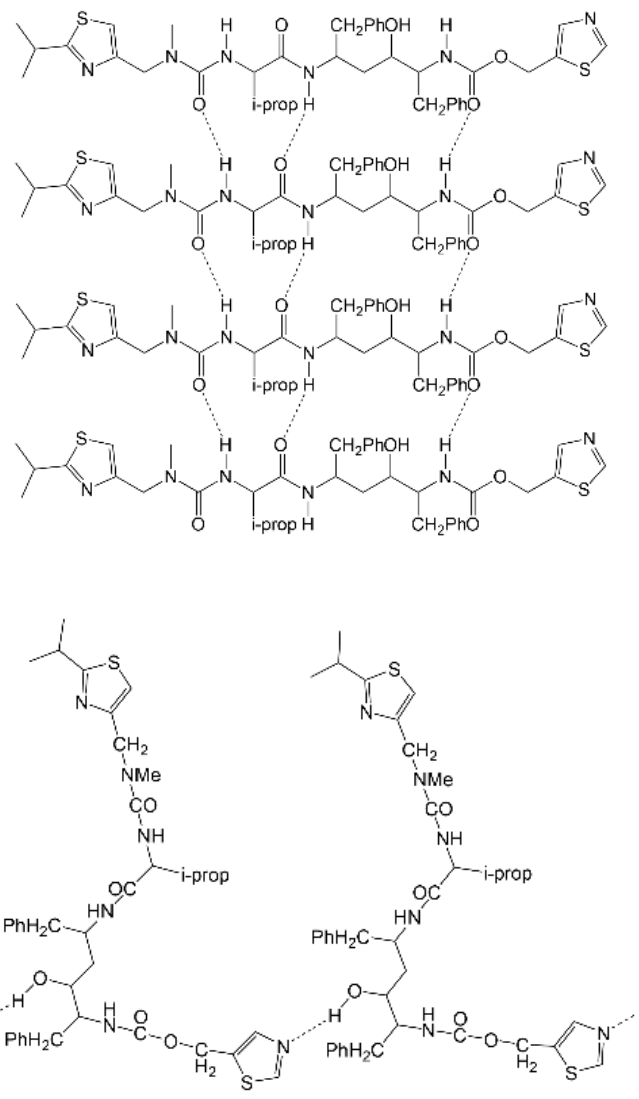

Form I

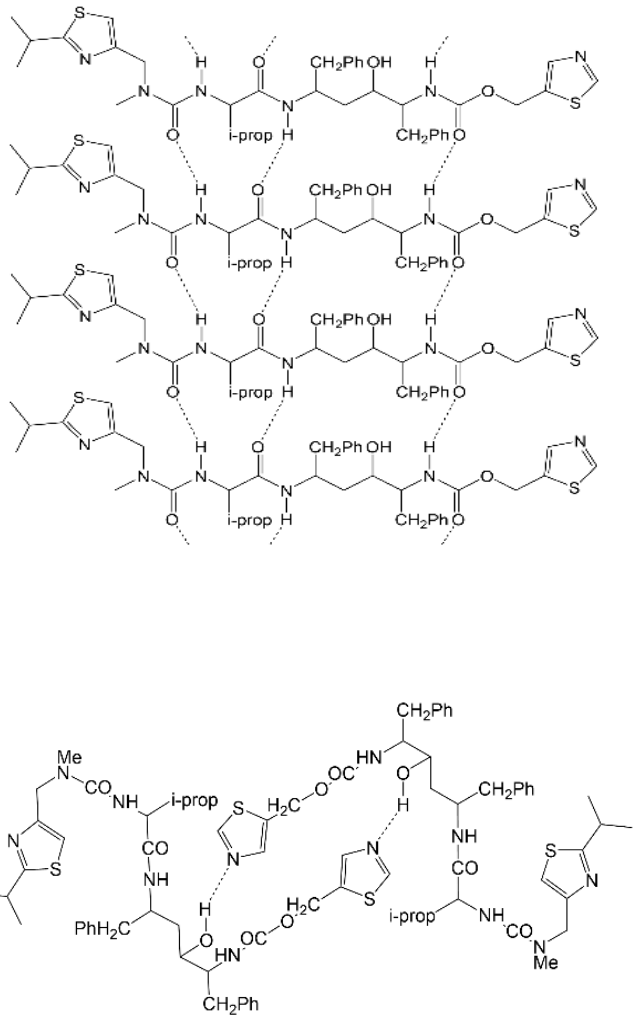

Form II

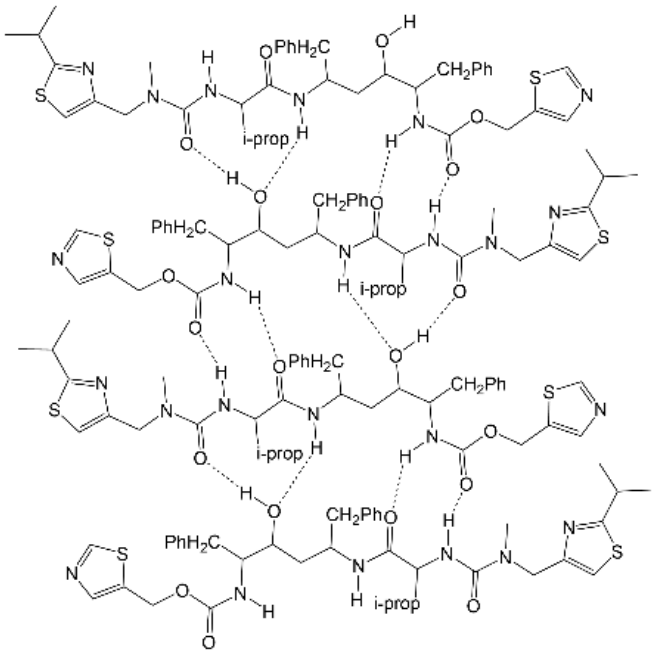

Table 3. Summary of hydrogen bonding parameters (D-A distances with Acceptors in Parenthesis)

	Donor Group			
	Amide	Carbamate	Urea	Alcohol
Form III	2.77(Amide)	2.80(Carbamate)	2.96, 2.97(Urea)	3.05, 3.69(Thiazole)
Form I	3.05(Amide)	3.18(Carbamate)	3.40(Urea)	3.04(Thiazole)
Form II	3.05(Alcohol)	2.89(Urea)	3.01(Carbamate)	2.69(Urea)

The crystal structure of Form III has been solved at two temperatures. We plot the density as a function of temperature in Figure 4c. The density of Form III is the lowest among the three RTV polymorphs, and has a similar thermal expansion coefficient (TEC) as Form I (Table 1). The lowest density is consistent with its lowest stability, according to Burger and Ramberger's Density Rule.[26]

Table 3 summarizes the H-bonding parameters in the three RTV polymorphs. Form III forms better H-bonds relative to Form I. Unlike the case of Form II, forming better H-bonds in Form III does not give higher stability than Form I, indicating the Density Rule[26] and the conformation energy may also play an important role.

Polymorphs of RTV raised the importance of polymorphism to an unprecedented level in the pharmaceutical industry. Although polymorphism of RTV has been studied for 30 years, a new polymorph can still be discovered from the melt. Considering many other examples,[14-16, 27] the importance of melt crystallization on polymorph screening cannot be ignored. We believe that melt crystallization is a promising approach to discover new polymorphs, especially for meta-stable polymorphs. From a thermodynamical point of view, the melt is more suitable for generating meta-stable polymorphs relative to solution crystallization. The melt is the most concentrated state and should have the highest driving force for crystallization and allow the existence of less stable polymorphs. Kinetically, polymorphs are competing in terms of crystal nucleation, crystal growth, and polymorph transition. Among the three factors, crystal nucleation likely plays the most important role in polymorphic selectivity. If the polymorphs can exist, the nucleation rates of the three forms in the melt and solution should decide the observed polymorph. Form III, the least stable form, likely can only be observed if it has the fastest nucleation rate. We will discuss the crystal nucleation of RTV Form III from its melt in detail later. Crystal growth is decided by molecular mobility under deep supercooling[28, 29] and has been found to be similar among the different polymorphs,[14, 30] and thus is unlikely to play an important role. Polymorphic transition

may be accelerated if both polymorphs nucleate concurrently and are in contact. The molten state is much more viscous than the solution state in general, and has much lower chance for the contact of different polymorphs, thus usually discourages polymorphic transition. When both polymorphs co-exist, the melt usually allows the observation of the less stable form more easily than solution state.

It is interesting that from the melt, in our study, only Form III nucleation occurs. This polymorph selectivity is consistent with the Ostwald Rule of Stages, the least stable polymorph nucleates first and then converts to the next least stable polymorph.[31] However, there are many reported exceptions to this rule.[32-34] Instead of using the Gibbs free energy as the predictor, Gui et al.[30] observed that the polymorphs with low density and high energy tend to nucleate first in several organic liquids (nifedipine, ROY, D-arabitol, and D-sorbitol) by plotting the relative lattice energy/density landscape. We plotted RTV landscape in the same way in Figure 7. The fastest-nucleating Form III in the melt is the least stable and the least dense polymorph, supporting the finding by Yue et al.[30]

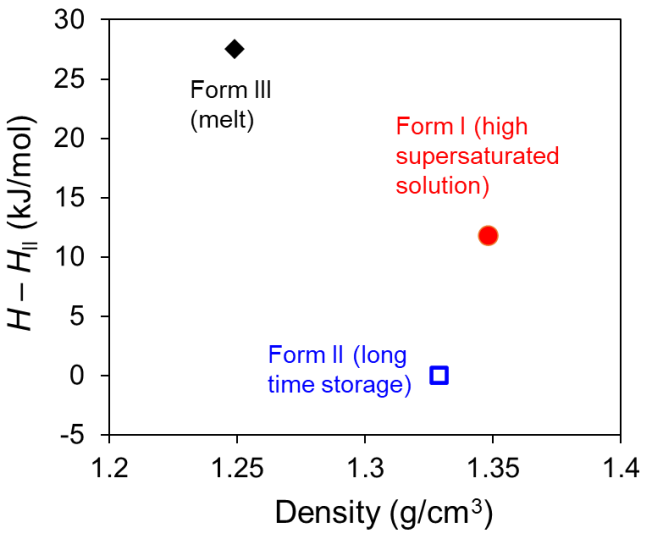

Figure 7. Relative lattice energy/density map of ritonavir polymorphs. The conditions of discovering the polymorphs are labeled.

The lesson learned from the discovery of RTV Form III is that studying crystal nucleation in the melt is important for polymorph screening workflow. RTV is a very flexible molecule and has slow crystallization kinetics due to its high flexibility.[35] Because of the slow nucleation rate, Form III can only be nucleated in a narrow range (60 – 70 °C) within a reasonable time (less than 1 week). When the nucleation rate is slow, it is very important to know the temperature having the highest nucleation rate in order to observe the initial crystals. Nucleation rates from the melt are usually fastest around 1.0 – 1.2 T_g according to the studied systems,[30, 33, 36-38] as shown in Figure 8. Glass transition temperature of RTV is 46 °C, measured by DSC at 10 °C/min heating rate. Thus, the temperatures with maximum nucleation rate (T_{max}, 60 – 70 °C) of RTV is around 1.04 – 1.08 T_g, consistent with the observations in other systems. Thus, a temperature range of

1.0 – 1.2 T_g can be used as a general guideline for studying crystal nucleation from the melt. By applying this rule of thumb, we successfully discovered RTV Form III, 24 years after the emergence of Form II. This demonstrated the importance of melt crystallization in discovering polymorphs, especially for flexible molecules with slow crystallization kinetics, like RTV.

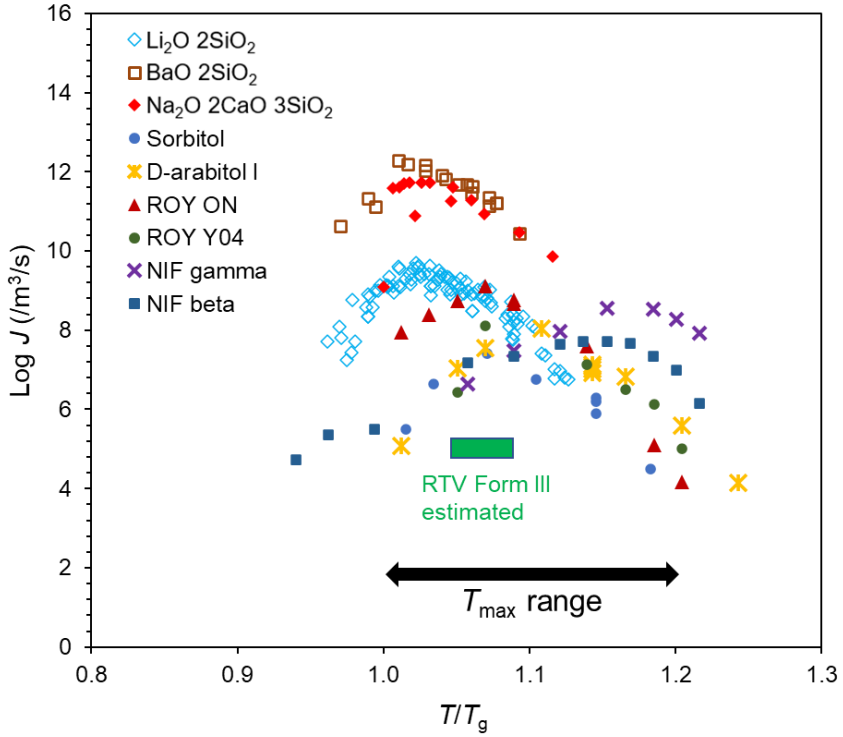

Figure 8. Nucleation rates of the studied systems as a function of T_g scaled temperature. T_{max} is within the range of 1.0 – 1.2 T_g in the studied systems to date.

CSP has been used to evaluate the risk of missing a more stable polymorph and predict possible new polymorphs in the pharmaceutical industry. CSP generally proceeds in three steps: (1) Exploring the energy-favorable conformations of target molecules. (2) Generating plausible crystal structures. (3) Ranking and optimizing the generated structures.[14, 22, 23] Additionally, from the simulated crystal structures, essential properties (e.g., solubility, log *P* and log *D*) can be calculated handily as a reference for nominating lead candidates.[39] Despite the advantages, for flexible molecules with many rotatable torsion angles, performing CSP is still very challenging due to the surge of conformations within local minima.[40] For a flexible molecule like RTV, current methods of CSP cannot be reduced to a reasonable cost,[40] and even calculating the energy landscape for a single molecule takes considerable computational sources.[41] In addition to its general flexibility, RTV Form II is known to exhibit a statistically rare conformation in its

carbamate group. This group would typically be treated as a rigid group in the more typical configuration in order to reduce the number of conformations that would need to be explored. However, fixing its conformation would make the discovery of the most stable form impossible by CSP. The case of RTV could be an ultimate test for CSP in the future. But for now, experimental approaches under diverse crystallization conditions remain the primary approaches for discovering crystal forms of large, flexible pharmaceuticals.

CONCLUSIONS

A new polymorph, Form III, of ritonavir was discovered via melt crystallization. Form III has a unique PXRD pattern, Raman spectrum, lower T_m , and H_m, compared to the know Form I and Form II. It is the least stable form, monotropically, among the three polymorphs. The three polymorphs have different conformations and hydrogen bonding motifs. Form III adopt the trans conformation in the N-methyl urea group of the 2,4-wing, as in Form II; trans conformation in carbamate group of the 5-wing, as in Form I, providing a good example of conformational polymorphism of a very flexible molecule. Form III can only be nucleated in a narrow temperature range (60 – 70 °C) in a reasonable experimental time due to its slow nucleation rate. This example demonstrates the importance of crystal nucleation studies. Crystallization from supercooled liquids should be incorporated as part of polymorph screening workflow.

ACKNOWLEDGEMENT

XY thank AbbVie Inc. for the internship opportunity.

DISCLOSURE

AbbVie participated in study design, research, data collection, analysis and interpretation of data, writing, reviewing, and approving the publication. XY, RFH and GGZZ are employees of AbbVie and may own AbbVie stock.

AUTHOR INFORMATION

Corresponding Author. Geoff G. Z. Zhang. Telephone: 847-937-4702. E-mail: Geoff.GZ.Zhang@abbvie.com.

REFERENCE

[1] J. Bernstein, Polymorphism in Molecular Crystals 2e, International Union of Crystal2020.
[2] H.G. Brittain, Polymorphism in pharmaceutical solids, Drugs and the pharmaceutical sciences, 95 (1999) 183-226.
[3] L. Yu, Polymorphism in molecular solids: an extraordinary system of red, orange, and yellow crystals, Accounts of chemical research, 43 (2010) 1257-1266.
[4] Y. Qiu, Y. Chen, G.G. Zhang, L. Yu, R.V. Mantri, Developing solid oral dosage forms: pharmaceutical theory and practice, Academic press2016.
[5] NORVIR® (ritonavir) Label: https://www.accessdata.fda.gov/drugsatfda_docs/label/2017/209512lbl.pdf.
[6] KALETRA® (lopinavir and ritonavir) Label: https://www.accessdata.fda.gov/drugsatfda_docs/label/2016/021251s052_021906s046lbl.pdf.
[7] APTIVUS® (tipranavir) Label: https://www.accessdata.fda.gov/drugsatfda_docs/label/2011/021814s011lbl.pdf.
[8] REYATAZ® (atazanavir) Label: https://www.accessdata.fda.gov/drugsatfda_docs/label/2016/021567s039,206352s004lbl.pdf.
[9] VIEKIRA PAK® (ombitasvir, paritaprevir, and ritonavir; dasabuvir) Label: https://www.accessdata.fda.gov/drugsatfda_docs/label/2014/206619lbl.pdf.
[10] PAXLOVIDTM (nirmatrelvir tablets; ritonavir tablets): https://www.fda.gov/media/155050/download.
[11] S.R. Chemburkar, J. Bauer, K. Deming, H. Spiwek, K. Patel, J. Morris, R. Henry, S. Spanton, W. Dziki, W. Porter, Dealing with the impact of ritonavir polymorphs on the late stages of bulk drug process development, Organic Process Research & Development, 4 (2000) 413-417.
[12] J. Bauer, S. Spanton, R. Henry, J. Quick, W. Dziki, W. Porter, J. Morris, Ritonavir: an extraordinary example of conformational polymorphism, Pharmaceutical research, 18 (2001) 859-866.
[13] S.L. Morissette, S. Soukasene, D. Levinson, M.J. Cima, Ö. Almarsson, Elucidation of crystal form diversity of the HIV protease inhibitor ritonavir by high-throughput crystallization, Proceedings of the National Academy of Sciences, 100 (2003) 2180-2184.
[14] C. Yao, I.A. Guzei, Y. Jin, S. Ruan, G. Sun, Y. Gui, L. Wang, L. Yu, Polymorphism of piroxicam: new polymorphs by melt crystallization and crystal structure Prediction, Crystal Growth & Design, 20 (2020) 7874-7881.
[15] N. Fellah, C.J. Zhang, C. Chen, C.T. Hu, B. Kahr, M.D. Ward, A.G. Shtukenberg, Highly Polymorphous Nicotinamide and Isonicotinamide: Solution versus Melt Crystallization, Crystal Growth & Design, 21 (2021) 4713-4724.
[16] Y. Gui, X. Yao, I.A. Guzei, M.M. Aristov, J. Yu, L. Yu, A Mechanism for Reversible Solid-State Transitions Involving Nitro Torsion, Chemistry of Materials, 32 (2020) 7754-7765.

[17] C.A. Mitchell, L. Yu, M.D. Ward, Selective nucleation and discovery of organic polymorphs through epitaxy with single crystal substrates, Journal of the American Chemical Society, 123 (2001) 10830-10839.
[18] C.P. Price, A.L. Grzesiak, A.J. Matzger, Crystalline polymorph selection and discovery with polymer heteronuclei, Journal of the American Chemical Society, 127 (2005) 5512-5517.
[19] M. Guerain, A review on high pressure experiments for study of crystallographic behavior and polymorphism of pharmaceutical materials, Journal of Pharmaceutical Sciences, 109 (2020) 2640-2653.
[20] J.-M. Ha, J.H. Wolf, M.A. Hillmyer, M.D. Ward, Polymorph selectivity under nanoscopic confinement, Journal of the American Chemical Society, 126 (2004) 3382-3383.
[21] X. Yao, Q. Liu, B. Wang, J. Yu, M.M. Aristov, C. Shi, G.G.Z. Zhang, L. Yu, Anisotropic Molecular Organization at a Liquid/Vapor Interface Promotes Crystal Nucleation with Polymorph Selection, Journal of the American Chemical Society (2022).
[22] A.M. Reilly, R.I. Cooper, C.S. Adjiman, S. Bhattacharya, A.D. Boese, J.G. Brandenburg, P.J. Bygrave, R. Bylsma, J.E. Campbell, R. Car, Report on the sixth blind test of organic crystal structure prediction methods, Acta Crystallographica Section B: Structural Science, Crystal Engineering and Materials, 72 (2016) 439-459.
[23] P. Zhang, G.P. Wood, J. Ma, M. Yang, Y. Liu, G. Sun, Y.A. Jiang, B.C. Hancock, S. Wen, Harnessing cloud architecture for crystal structure prediction calculations, Crystal Growth & Design, 18 (2018) 6891-6900.
[24] X. Ou, X. Li, H. Rong, L. Yu, M. Lu, A general method for cultivating single crystals from melt microdroplets, Chemical Communications, 56 (2020) 9950-9953.
[25] X. Yao, E.G. Benson, Y. Gui, T. Stelzer, G.G. Zhang, L. Yu, Surfactants Accelerate Crystallization of Amorphous Nifedipine by Similar Enhancement of Nucleation and Growth Independent of Hydrophilic–Lipophilic Balance, Molecular Pharmaceutics, (2022).
[26] A. Burger, R. Ramberger, On the polymorphism of pharmaceuticals and other molecular crystals. I, Microchimica Acta, 72 (1979) 259-271.
[27] X. Zhu, C.T. Hu, B. Erriah, L. Vogt-Maranto, J. Yang, Y. Yang, M. Qiu, N. Fellah, M.E. Tuckerman, M.D. Ward, Imidacloprid crystal polymorphs for disease vector control and pollinator protection, Journal of the American Chemical Society, 143 (2021) 17144-17152.
[28] C. Huang, S. Ruan, T. Cai, L. Yu, Fast surface diffusion and crystallization of amorphous griseofulvin, The Journal of Physical Chemistry B, 121 (2017) 9463-9468.
[29] M.D. Ediger, P. Harrowell, L. Yu, Crystal growth kinetics exhibit a fragility-dependent decoupling from viscosity, The Journal of chemical physics, 128 (2008) 034709.
[30] Y. Gui, C. Huang, C. Shi, G.G.Z. Zhang, L. Yu, Polymorphic Selection in Crystal Nucleation, The Journal of chemical physics, doi: 10.1063/5.0086308 (2022).
[31] W. Ostwald, Studien über die Bildung und Umwandlung fester Körper, Zeitschrift für physikalische Chemie, 22 (1897) 289-330.
[32] L.S. Germann, M. Arhangelskis, M. Etter, R.E. Dinnebier, T. Friščić, Challenging the Ostwald rule of stages in mechanochemical cocrystallisation, Chemical science, 11 (2020) 10092-10100.
[33] C. Huang, Z. Chen, Y. Gui, C. Shi, G.G. Zhang, L. Yu, Crystal nucleation rates in glass-forming molecular liquids: D-sorbitol, D-arabitol, D-xylitol, and glycerol, The Journal of chemical physics, 149 (2018) 054503.
[34] L.O. Hedges, S. Whitelam, Limit of validity of Ostwald's rule of stages in a statistical mechanical model of crystallization, The Journal of chemical physics, 135 (2011) 164902.

[35] D. Zhou, E.A. Schmitt, D. Law, P.J. Brackemeyer, G.G. Zhang, Assessing physical stability risk using the amorphous classification system (ACS) based on simple thermal analysis, Molecular Pharmaceutics, 16 (2019) 2742-2754.
[36] K.F. Kelton, Crystal nucleation in liquids and glasses, Solid state physics, Elsevier1991, pp. 75-177.
[37] K.L. Narayan, K.F. Kelton, First measurements of time-dependent nucleation as a function of composition in Na2O· 2CaO· 3SiO2 glasses, Journal of non-crystalline solids, 220 (1997) 222-230.
[38] P.K. Gupta, D.R. Cassar, E.D. Zanotto, Role of dynamic heterogeneities in crystal nucleation kinetics in an oxide supercooled liquid, The Journal of Chemical Physics, 145 (2016) 211920.
[39] R.S. Hong, A. Mattei, A.Y. Sheikh, R.M. Bhardwaj, M.A. Bellucci, K.F. McDaniel, M.O. Pierce, G. Sun, S. Li, L. Wang, Novel physics-based ensemble modeling approach that utilizes 3D molecular conformation and packing to access aqueous thermodynamic solubility: A case study of orally available bromodomain and extraterminal domain inhibitor lead optimization series, Journal of Chemical Information and Modeling, 61 (2021) 1412-1426.
[40] S.L. Price, D.E. Braun, S.M. Reutzel-Edens, Can computed crystal energy landscapes help understand pharmaceutical solids?, Chemical Communications, 52 (2016) 7065-7077.
[41] D. Chakraborty, N. Sengupta, D.J. Wales, Conformational energy landscape of the ritonavir molecule, The Journal of Physical Chemistry B, 120 (2016) 4331-4340.

For TOC only